

# Large-Scale Synthesis of Ultrathin Bi<sub>2</sub>S<sub>3</sub> Necklace Nanowires\*\*

Ludovico Cademartiri, Reihaneh Malakooti, Paul G. O'Brien, Andrea Migliori, Srebri Petrov, Nazir P. Kherani, and Geoffrey A. Ozin\*

One of the most fascinating areas of nanoscience is the study of one-dimensional nanostructures.<sup>[1]</sup> From our materials chemistry viewpoint the idea of bringing the size of nanowires down to a point where nanoscale colloidal analogues of polymers can be studied is most stimulating. This direction has been the subject of intense study that promises to develop a new class of materials in which the topological properties of polymers can be coupled with quantum size effects and inorganic crystalline materials.<sup>[2,3]</sup> Our strategy goes in a singular direction: instead of connecting nanocrystals by ligand chemistry<sup>[4]</sup> or dipole interactions<sup>[5]</sup> we aim to synthesize colloidal nanowires thin enough to display polymer-like behavior.

Colloidal chemistry has in recent years shown that virtually any composition can be obtained as colloidal nanocrystals of the most diverse shapes.<sup>[6]</sup> Much work though still needs to be done in the area of pnictide chalcogenides for which very few syntheses are available for obtaining colloidal stable products<sup>[7–10]</sup> and none to our knowledge has shown fully demonstrated quantum size effects. Pnictide chalcogenides (Bi<sub>2</sub>S<sub>3</sub> in particular) are in fact known to show extremely wide changes in the bandgap energy and conductivity with changes in stoichiometry.<sup>[11,12]</sup>

In the present work we report a “low”-temperature, gram-scale route to Bi<sub>2</sub>S<sub>3</sub> nanowires of unprecedented thickness (<2 nm), with a necklace architecture, strong excitonic features never before seen in bismuth chalcogenides, and extremely high extinction coefficients. The wires are colloidal stable for months even after extensive purification.

The nanowires were obtained by injecting a solution of sulfur in oleylamine into a saturated solution of bismuth citrate in oleylamine at 130 °C (see Supporting Information). The nanowires start nucleating immediately after injection and are shown in Figure 1a. The wires are below 2 nm in diameter and display remarkable size uniformity as well as a lack of extensive branching (even though branching points can be seldomly observed). The length of the wires could not be measured rigorously due to their melting under e-beam irradiation, but light scattering measurements indicate their length can be in the order of several microns. Strikingly, the diameter of the wires does not change during growth (Supporting Information), as it will be later shown. In Figure 1b we show a Z-contrast TEM image, which indicates the melting the wires undergo upon e-beam irradiation. The inhomogeneity in the droplet spacing is a hint to the nanowire's texture that will be highlighted later.

The HRTEM image obtained from the wires (Figure 1c) shows some slightly elongated nanocrystals. The fact that only certain parts of the wires show lattice fringes at a given time indicates their polycrystalline microstructure. The lattice spacing that is evidenced in Figure 1c corresponds to the (021) planes of the Bi<sub>2</sub>S<sub>3</sub> structure.

The reaction is highly scalable due to the high concentration of the reagents and its high yield (>60%): multigram quantities can be routinely obtained in a laboratory environment. Figure 1d depicts over 17 grams of nanowires produced in the course of a single reaction (ca. 350 mL).

Unlike for single-crystalline ultrathin nanowires,<sup>[13–15]</sup> the powder X-ray diffraction (XRD) pattern for the Bi<sub>2</sub>S<sub>3</sub> nanowires (Figure 2a) is devoid of relatively sharp features, which seems to indicate a rather isotropic nanocrystalline component. In ultrathin nanowires, the different coherence lengths along the different crystallographic directions, which are due to the high aspect ratio and small size, give rise to sharp peaks on a broad background.<sup>[13–15]</sup> In this case, the XRD pattern is more consistent with a spherical nanocrystal system: Rietveld refinement of the XRD pattern was successfully accomplished by using the Bi<sub>2</sub>S<sub>3</sub> unit cell as well as a spherical particle model with a 1.6 nm size, consistent with the microscopy data (Supporting Information). It is important here not to overestimate the accuracy of Rietveld refinement when it comes to nanocrystal shape determination but it is safe to say that we are not dealing with a one-dimensional single crystal.

[\*] L. Cademartiri, R. Malakooti,<sup>[†]</sup> Dr. S. Petrov, Prof. G. A. Ozin  
Lash Miller Chemical Laboratories  
Department of Chemistry, University of Toronto  
80 St. George Street, Toronto, ON, M5S 3H6 (Canada)  
Fax: (+1) 416-971-2011  
E-mail: gozin@chem.utoronto.ca  
Homepage: <http://www.chem.toronto.edu/staff/GAO/group.html>  
P. G. O'Brien, Prof. N. P. Kherani  
Department of Materials Science and Engineering  
University of Toronto  
184 College Street, Toronto, ON, M5S 3E4 (Canada)  
Dr. A. Migliori  
Consiglio Nazionale delle Ricerche, CNR-IMM  
Area della Ricerca di Bologna  
Via Gobetti 101, 40126 Bologna (Italy)  
Prof. N. P. Kherani  
Department of Electrical and Computer Engineering  
University of Toronto  
10 King's College Road, Toronto, ON, M5S 3G4 (Canada)

[†] present address: Department of Chemistry  
University of Birjand, Birjand, South Khorasan (Iran)

[\*\*] G.A.O. is Canada Research Chair in Materials Chemistry. The authors are deeply indebted to the NSERC for financial support. L.C. thanks the University of Toronto for a scholarship. R.M. thanks the Iranian Ministry of Science, Research and Technology for a scholarship and F. Farzaneh for support

Supporting information for this article is available on the WWW under <http://www.angewandte.org> or from the author.

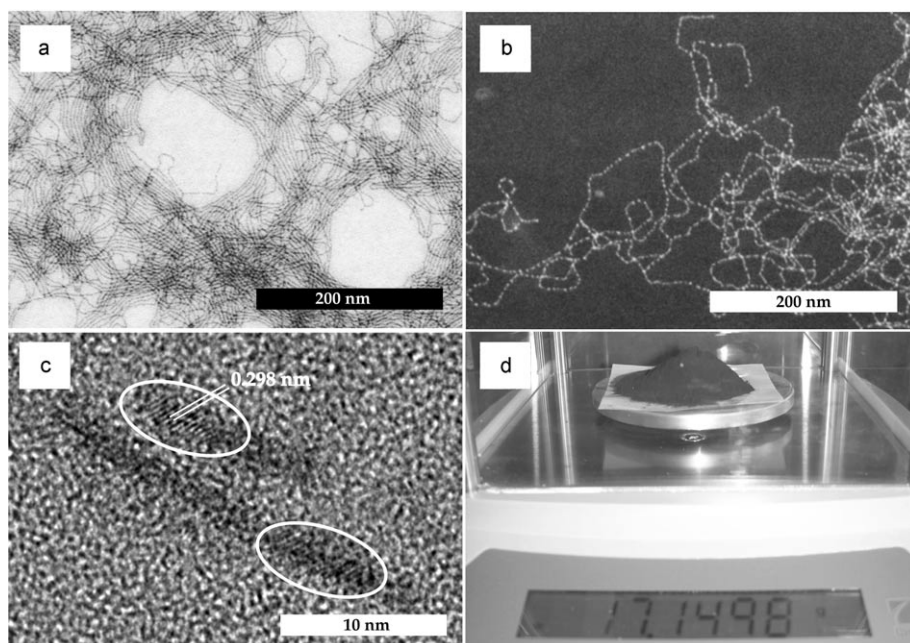


**Figure 1.** Microscopic characterization of  $\text{Bi}_2\text{S}_3$  necklace nanowires. TEM (a) and ZC-TEM (b) of the  $\text{Bi}_2\text{S}_3$  nanowires deposited on a carbon coated grid; c) HRTEM of nanowire fragments—the ellipses highlight the areas of the wire where the orientation of the crystalline lattice of the nanocrystals is parallel to the beam—the lattice spacing of 0.298 nm highlighted in the Figure corresponds to (021) planes of the  $\text{Bi}_2\text{S}_3$  structure; d) demonstration of ultralarge scale synthesis obtained from a  $\approx 350$  mL reaction: the wires depicted have been stripped off the ligand by hydrazine treatment.

Reasonably strong variations in nanocrystal size and shape can also be expected: for example, the nanocrystals shown in Figure 1c are elongated to about 5 nm along the wire. We think—and the HRTEM and SAED investigations support this idea—that this anomalous elongation allowed them to resist e-beam irradiation without melting due to the greater-than-average crystal volume. The elongated shape is not the result of melting-recrystallization, as the melt forms spherical droplets (Supporting Information), especially considering the very high hydrophobicity which is expected of such a fluid.

Absorption spectroscopy allowed us to characterize the quantum confinement effects in the wires. The UV/Vis absorption spectrum of a representative sample is shown in Figure 2b. A second derivative analysis of various spectra from different samples allowed us to identify three peaks within the band-edge absorption background. To claim that the peaks are indeed due to quantum confinement effects, an at least qualitative agreement with the effective mass approximation (EMA) theory should be expected. Given the extremely small size of the wires, the sensitivity to the e-beam, and the consequent inaccuracy in the size determination, we relied on a test which would only rely on spectral features.<sup>[16]</sup> If one plots the normalized confinement energies (NCE) of the  $x$  transition (defined as  $(E_x - E_g)/(E_1 - E_g)$ ) as a function of the confinement energy of the first transition one obtains the NCE plot. According to the EMA, the NCE should be independent of the confinement energy of the first transition thus giving a straight horizontal line on the NCE plot.<sup>[17]</sup> As shown in Figure 2c, the NCE from the second and third transitions are approximately constant, suggesting that

we are indeed observing quantum confinement effects. The unprecedented oscillator strengths of these transitions also strongly suggest that we are facing a case of three-dimensional quantum confinement instead of the two-dimensional quantum confinement expected for nanowires. This is the first time that excitonic features are clearly identified in bismuth chalcogenides at room temperature, and this is likely due to the fact that structures of this size and shape were never obtained before. The only model that justifies all the observed data is a necklace model in which  $\text{Bi}_2\text{S}_3$  nanocrystals of approximately spherical shape are separated within the wire by amorphous regions or grain boundaries. Monitoring the excitonic features during nanowire growth confirmed that the nanowires do not grow in thickness in the reported conditions: the excitonic peaks remained virtually unchanged during the entire course of a 3 h reaction (Supporting Information).

At this point any statements on the possible growth mechanism of the wires would be premature. One can though speculate that we are not dealing with an oriented attachment mechanism, as the wires are not single crystals. The stability in thickness during the reaction also seems to indicate that at about 1.6 nm the ribbonlike structure of  $\text{Bi}_2\text{S}_3$  reaches a stable configuration, much like in magic clusters, such that any further growth in thickness is unfavored at least in these thermodynamic conditions. The presence of such a minimal building block is further corroborated by the observation of very similarly sized nanostructures in the isostructural and chemically similar  $\text{Sb}_2\text{S}_3$ .<sup>[15,18]</sup> The mechanism by which these building blocks attach forming nearly periodical interfaces is unknown.

A material property that is of fundamental importance for practical and theoretical purposes is the extinction coefficient. Compared to spherical nanocrystals, the particularly challenging aspect of measuring this quantity in these nanostructures lies in the difficulty in determining their size with enough accuracy. We thus decided to express the extinction coefficient in terms of bismuth concentration.

The amount of bismuth was measured by two independent techniques: inductively coupled plasma atomic emission spectroscopy (ICP-AES) and thermogravimetric analysis (TGA). The resulting value of extinction coefficient from both techniques is plotted in Figure 2d and the relatively small difference between the two curves gives an idea of the error that has to be taken into account in this sort of measurements.<sup>[19,20]</sup> The extinction coefficient per cation at 500 nm was found to exceed  $7400 \text{ M}^{-1} \text{ cm}^{-1}$ , nearly an order of

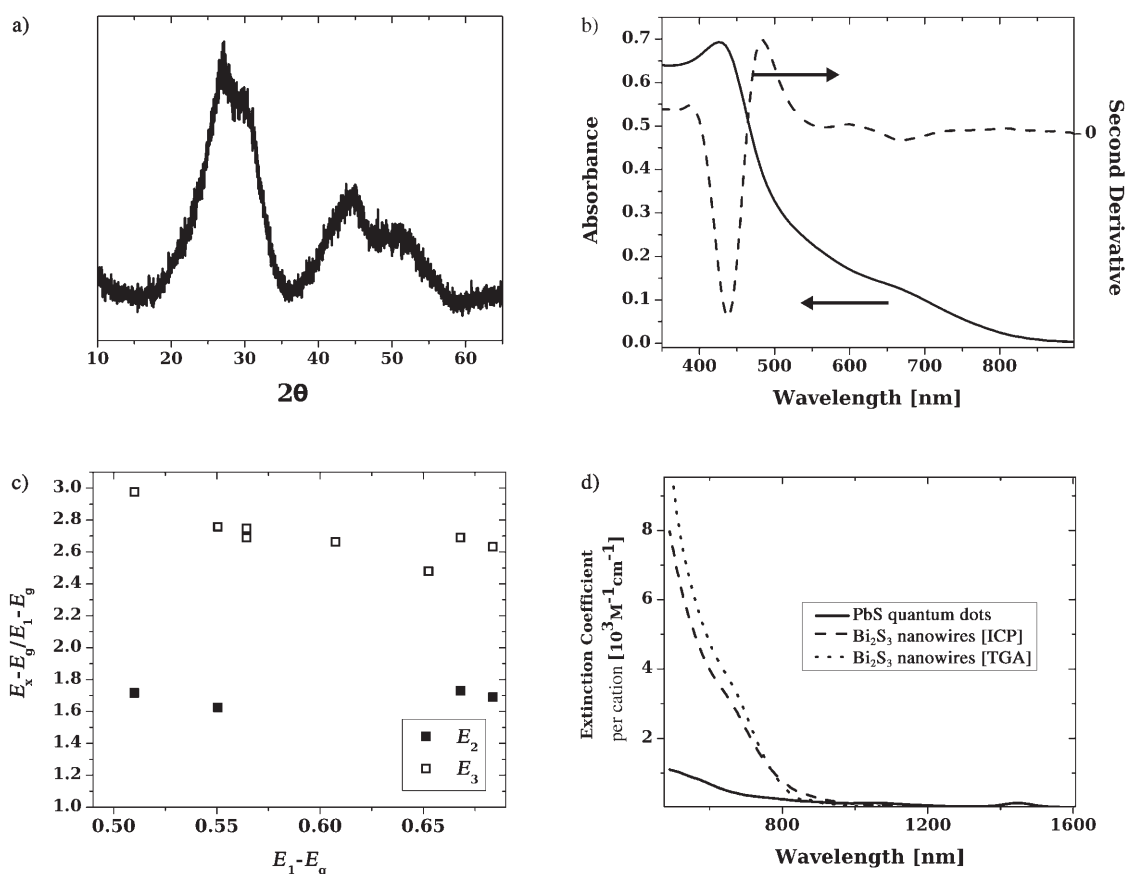


**Figure 2.** Optical and structural characterization of the  $\text{Bi}_2\text{S}_3$  necklace nanowires; a) XRD pattern of the purified  $\text{Bi}_2\text{S}_3$  nanowires; b) UV/Vis absorption spectrum (solid) and its second derivative (dashed) of a solution of  $\text{Bi}_2\text{S}_3$  nanowires showing the occurrence of three separate transitions; c) normalized confinement energy plot of the three transitions consistent with the effective mass approximation theory; d) per cation extinction coefficient of PbS quantum dots and  $\text{Bi}_2\text{S}_3$  nanowires, measured by ICP and TGA.

magnitude higher than what we observed in PbS nanocrystal quantum dots, which are known for their high extinction coefficient.<sup>[20]</sup> This result is somewhat unexpected since  $\text{Bi}_2\text{S}_3$  has a considerably larger bandgap than PbS (1.3 eV vs. 0.41 eV) and a comparable refractive index<sup>[21]</sup> ( $\approx 4$ ). The reason might lie in the giant oscillator strength effect predicted by the EMA which has thus not been observed consistently in quantum dot systems.<sup>[19,20,22,23]</sup> This effect predicts that the oscillator strength (per volume) of optical transitions in semiconductors would be proportional to  $r^{-3}$  and thus would justify such a strong oscillator strength in such diminutive structures as the ones we report here.<sup>[24]</sup>

While single-wire measurements are beyond the scope of this report, the electrical properties of  $\text{Bi}_2\text{S}_3$  nanowire films could be easily measured and the results are shown in Figure 3. To obtain these results  $\text{Bi}_2\text{S}_3$  nanowire films were spin-coated onto highly resistive glass slides, and two square co-planar aluminum contacts ( $1\text{ cm}^2$ ), spaced apart by 1 mm, were subsequently deposited by physical vapor deposition onto these films. The current through these films was then measured as different biases were applied across the pair of aluminum contacts. As shown in Figure 3a the films were found to be insulating due to the large interwire distance, which is determined by the length of the oleylamine molecules ( $\approx 2\text{ nm}$ ): a 5 min treatment with 1M hydrazine

solution in THF increased the conductivity of the films by three orders of magnitude, consistent with the results obtained on PbSe nanocrystal films.<sup>[25]</sup> The conductivity of the films after such short treatment in hydrazine was found to be about  $4 \times 10^{-5}\text{ S cm}^{-1}$ . Longer treatments in hydrazine were found to crack the films due to the shrinkage consequent to the replacement of oleylamines with short hydrazine molecules. Repeated deposition and hydrazine treatment cycles did not seem to completely solve this issue. Ligands shorter than oleylamine might need to be used to minimize such shrinking upon hydrazine exposure.

The temperature dependence of the conductivity shows that the nanowire films are semiconducting (Figure 3b). The conductivity increases exponentially with temperature analogously to that previously reported for  $\text{Bi}_2\text{S}_3$  thin films and nanowires.<sup>[12,26]</sup> The spectral dependence of the photoconductivity is shown in Figure 3c and compared to the absorbance spectrum. The close resemblance of the two curves proves that the photogenerated carriers are indeed originating from quantum confined excitons generated within the nanowires.<sup>[27]</sup>

In conclusion, we have demonstrated a facile and green route to the gram-scale preparation of colloiddally stable ultrathin  $\text{Bi}_2\text{S}_3$  nanowires showing quantum confinement effects and a necklace architecture. Nanostructures such as

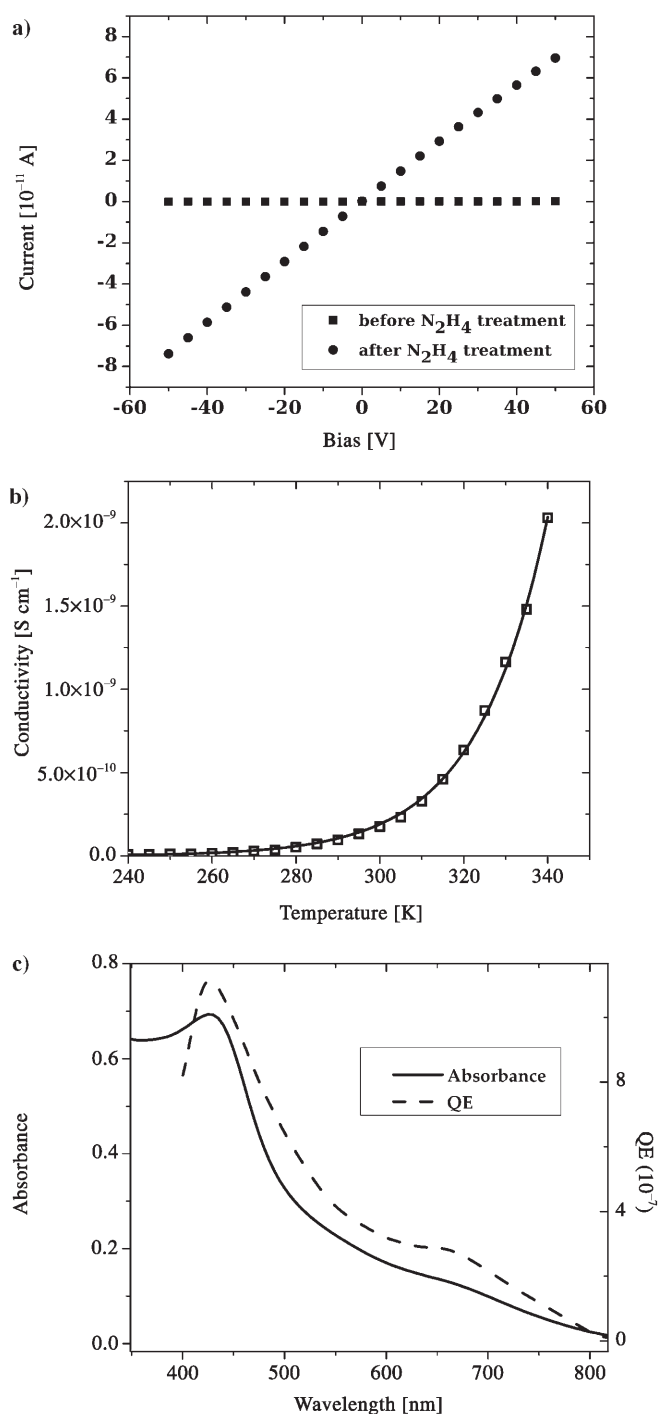


**Figure 3.** Electrical conductivity of  $Bi_2S_3$  nanowire films; a) IV curves of  $Bi_2S_3$  nanowire films before and after hydrazine treatment. The increase of three orders of magnitude in the conductivity is due to the reduction of the distance between the wires caused by the exchange of the original bulky capping ligand with the short hydrazine molecules; b) temperature dependence of conductivity; c) spectral response of photoconductivity (dashed line) compared to absorbance spectrum.

these are in our opinion of fundamental scientific interest and of very high technological potential for thermoelectric applications.

Received: October 30, 2007

Revised: February 4, 2008

Published online: April 9, 2008

**Keywords:** bismuth · colloids · nanostructures · nanowires · quantum confinement

- [1] Y. N. Xia, P. D. Yang, Y. G. Sun, Y. Y. Wu, B. Mayers, B. Gates, Y. D. Yin, F. Kim, Y. Q. Yan, *Adv. Mater.* **2003**, *15*, 353.
- [2] Z. Y. Tang, N. A. Kotov, *Adv. Mater.* **2005**, *17*, 951.
- [3] R. L. Penn, *J. Phys. Chem. B* **2004**, *108*, 12707.
- [4] G. A. DeVries, M. Brunnbauer, Y. Hu, A. M. Jackson, B. Long, B. T. Neltner, O. Uzun, B. H. Wunsch, F. Stellacci, *Science* **2007**, *315*, 358.
- [5] K.-S. Cho, D. V. Talapin, W. Gaschler, C. B. Murray, *J. Am. Chem. Soc.* **2005**, *127*, 7140.
- [6] Y. Yin, A. P. Alivisatos, *Nature* **2005**, *437*, 664.
- [7] M. B. Sigman, Jr., B. A. Korgel, *Chem. Mater.* **2005**, *17*, 1655.
- [8] R. Malakooti, L. Cademartiri, Y. Akcikir, S. Petrov, A. Migliori, G. A. Ozin, *Adv. Mater.* **2006**, *18*, 2189.
- [9] B. F. Variano, D. M. Hwang, C. J. Sandroff, P. Wiltzius, T. W. Jing, N. P. Ong, *J. Phys. Chem.* **1987**, *91*, 6455.
- [10] P. Christian, P. O'Brien, *J. Mater. Chem.* **2005**, *15*, 3021.
- [11] M. E. Rincón, M. Sanchez, P. J. George, A. Sanchez, P. K. Nair, *J. Solid State Chem.* **1998**, *136*, 167.
- [12] A. D. Schriker, M. B. Sigman, B. A. Korgel, *Nanotechnology* **2005**, *16*, S508.
- [13] Z. P. Liu, D. Xu, J. B. Liang, J. M. Shen, S. Y. Zhang, Y. T. Qian, *J. Phys. Chem. B* **2005**, *109*, 10699.
- [14] T. Yu, J. Joo, Y. I. Park, T. Hyeon, *J. Am. Chem. Soc.* **2006**, *128*, 1786.
- [15] R. Malakooti, L. Cademartiri, A. Migliori, G. A. Ozin, *J. Mater. Chem.* **2008**, *18*, 66.
- [16] B. L. Wehrenberg, C. J. Wang, P. Guyot-Sionnest, *J. Phys. Chem. B* **2002**, *106*, 10634.
- [17] J. Black, E. M. Conwell, L. Seigle, C. W. Spencer, *J. Phys. Chem. Solids* **1957**, *2*, 240.
- [18] K. H. Park, J. Choi, H. J. Kim, J. B. Lee, S. U. Son, *Chem. Mater.* **2007**, *19*, 3861.
- [19] W. W. Yu, L. Qu, W. Guo, X. Peng, *Chem. Mater.* **2003**, *15*, 2854.
- [20] L. Cademartiri, E. Montanari, G. Calestani, A. Migliori, A. Guagliardi, G. A. Ozin, *J. Am. Chem. Soc.* **2006**, *128*, 10337.
- [21] A. Cantarero, J. P. Martinez, A. Segura, A. Chevy, *Phys. Status Solidi A* **1987**, *101*, 603.
- [22] P. R. Yu, M. C. Beard, R. J. Ellingson, S. Ferrere, C. Curtis, J. Drexler, F. Luiszer, A. J. Nozik, *J. Phys. Chem. B* **2005**, *109*, 7084.
- [23] C. A. Leatherdale, W. K. Woo, F. V. Mikulec, M. G. Bawendi, *J. Phys. Chem. B* **2002**, *106*, 7619.
- [24] Y. Wang, N. Herron, *J. Phys. Chem.* **1991**, *95*, 525.
- [25] D. V. Talapin, C. B. Murray, *Science* **2005**, *310*, 86.
- [26] M. Medles, N. Benramdane, A. Bouzidi, A. Nakrela, H. Tabet-Derraz, Z. Kebbab, C. Mathieu, B. Khelifa, R. Desfeux, *Thin Solid Films* **2006**, *497*, 58.
- [27] C. A. Leatherdale, C. R. Kagan, N. Y. Morgan, S. A. Empedocles, M. A. Kastner, M. G. Bawendi, *Phys. Rev. B* **2000**, *62*, 2669.